# An integral augmented sliding mode controller: the experimental application to level control plant


## Ajit Rambhau Laware*

Department of Electrical Engineering,
Dr. Vithalrao Vikhe Patil College of Engineering,
Ahmednagar, India
and
Savitribai Phule Pune University,
Pune, India
Email: ajitlaware2003@gmail.com
*Corresponding author

## Bhagsen Jaggnath Parvat

Department of Instrumentation and Control Engineering,
Karmaveer Adv. Baburao Thakare,
College of Engineering,
Nashik, India
Email: pbhagsen@yahoo.com

## Ravindra Rambhau Navthar

Department of Mechanical Engineering,
Dr. Vithalrao Vikhe Patil College of Engineering,
Ahmednagar, India
Email: navthar.mech@enggnagar.com


**Abstract:** It is well-known that servo and regulatory problems in industrial applications requires zero steady-state error. In the absence of an integral-action, uncontrolled systems give steady-state error to some extent or degraded performance under parametric uncertainties and bounded disturbances. Hence, real-time experimentation with integral augmented sliding mode control (IASMC) is adopted to enhance the closed-loop performance of level control plant. Lyapunov candidate function ensures the stability of a system. The practicability of IASMC is guaranteed with laboratory level control model. Experimental results obtained are compared with conventional sliding mode control (SMC) strategies reported by earlier researchers, and proportional-integral-derivative (PID) controller. An evaluation of experimental results with the assumption that nominal plant dynamics are known reveals that the proposed control design method provides a better set-point tracking performance, and fast and smooth level regulation in the presence of external bounded disturbances. It shows better time-domain specifications and error-based performance indices. The study shows that IASMC is applicable to industrial control systems and an alternate control strategy to prevalent design methods.

**Keywords:** integral control; PID control; real-time experimentation; sliding mode control.

**Reference** to this paper should be made as follows: Laware, A.R., Parvat, B.J. and Navthar, R.R. (2024) 'An integral augmented sliding mode controller: the experimental application to level control plant', *Int. J. Automation and Control*, Vol. 18, No. 4, pp.385–407.

**Biographical notes:** Ajit Rambhau Laware received his BE in Instrumentation and Control Engineering from the Government College of Engineering, Jalgaon, India in 2000 and ME in Instrumentation and Control Engineering from the Pune University in 2007. He completed his PhD in Electrical Engineering from the Pune University, Pune, India in 2020. His research interests include control system design, sliding mode controller synthesis, and its optimisation.

Bhagsen Jaggnath Parvat is currently the Head and an Associated Professor of the Instrumentation and Control Engineering Department in the KBT College of Engineering, Nashik. He received his undergraduate degrees as well as his MTech from the University of Pune. His PhD is in Instrumentation and Control Engineering from the SRTM University, Nanded, and areas of interest are control systems and process instrumentation. He has published a number of papers in preferred journals and chapters in books. Also, he presented various academic as well as research-based papers at several national and international conferences.

Ravindra Rambhau Navthar is currently a Professor in Mechanical Engineering Department at the Dr. Vithalrao Vikhe Patil College of Engineering, Ahmednagar, Maharashtra, India. He received his Bachelor's in Mechanical Engineering and Master's in Design Engineering from the Pravara Rural Engineering College (Savitribai Phule Pune University, Pune). He has received PhD in Mechanical Engineering from the North Maharashtra University in 2016. He has teaching experience of 22 years and has published 50+ papers in reputed international journals. His research areas are tribology, fluid dynamics, artificial neural networks, and control systems.

## 1 Introduction

Proportional, integral and derivative (PID) controller gains popularity and acceptance for control in process industries due to easy implementation in hardware (through filters, microcontrollers, programmable logic controllers, etc.), efficiency and robust nature against some common uncertainties (Karanam and Shaw, 2022). However, due to 'variability' of process parameters, the plant cannot work under set equilibrium condition and control performance index will get deviate. PID controller cannot incorporate ramp-type input and slow disturbances. An inclusion of integral-action reduces steady-state error but it increases over adjustment. Again, the control efforts of classical PID controller may not be good enough for non-linear, time-delay and complex processes with uncertain parameters.

The different control design methods were proposed by researchers to handle above stated issues. Particle swarm optimisation-based internal model control-PID was designed for magnetic levitation system in which the parameters were calculated using Maclaurin series expansion. Real-time experimentation shows the effectiveness of proposed strategy in terms of transient and tracking responses (Pati and Negi, 2019).

The repercussion of these drawbacks can be reduced by non-linear robust control methods (Joseph et al., 2022; Flores-Guerrero et al., 2021). The Quantitative feedback theory-based robust controller was designed for twin rotor control system with decoupled strategy. They compared the result with classical PID controller using simulation tests (Sharma and Pratap, 2020) while Pilla et al. (2021) explored observer-based state feedback controller in inner-loop for speed control of permanent magnet synchronous motor. They synthesised PI controller in outer-loop. The presented work cancel out nonlinearities and makes the system more stable. The validation of proposed method was done via simulation and experimental tests using dSPACE DS1103 controller board.

An optimal self-tuning interval type-2 fuzzy PI controller was demonstrated for precise positioning of the actuator to achieve desired performance. Authors compared the performance with prevalent methods through simulation results whille an experimental study was carried out on DC servo position control system. Lyapunov-based stability analysis was performed (De Maity et al., 2022). Wu and Zhao (2023) designed Lyapunov-based model predictive control strategy to a chemical process for achieveing satisfactory performance. The error-trigering technique was used to validate the proposed strategy via simulation tests.

Sliding mode control (SMC) is the richest non-linear robust control strategy as it shows invariance against perturbations and external bounded disturbances when system trajectories reside on the sliding manifold (Abdelhedi and Derbel, 2019). SMC possess many advantages:

1 insensitivity to perturbations of the system parameters

2 bounded and external disturbance suppression/rejection

3 better transient response

4 fast dynamic response

5 finite-time stability (Castellanos-Cardenas et al., 2022; Siddiqui et al., 2020; Utkin et al., 2020).

The dynamic response under SMC can be altered using an appropriate selection of discontinuous function (Wu et al., 2022).

System performance strongly depends on proper choice of sliding variables and control law parameters. Fine-tuning of parameters enable alleviation of tracking error and deviation in steady-state condition to a desired level in real-time applications. The selection of gain coefficient is time-consuming and complicated. Several trials have to conduct for finding optimum values (Toshani and Farrokhi, 2017). Unfortunately, due to discontinuous signal in ideal SMC, infinitely fast switching causes premature wear and tear of an actuator (Laware et al., 2023a). Such discontinuous function produces ‘chattering’. To counteract this limitation in SMC, an approximation of discontinuity has been considered by replacing ‘sgn’ function with a ‘sigmoid’ function (Utkin et al., 2020).

Several researchers have tried to alleviate the chattering phenomena in practical applications (Laware et al., 2022; Mat-Noh et al., 2019). Samira and Renuganth (2017) explored integral augmented sliding mode controller (IASMC) with boundary-layer technique to improve steady-state precision attitude-tracking system. They have shown that SMC with integral-action provides better results than classical controllers for attitude control problem. Lamzouri et al. (2022) presented a novel strategy of output power control of an electric generation system with battery bank and variable load using integral action in switching surface. The numerical simulations demonstrates improved transient response with minimised steady state error.

The set-point regulation problem using conditional integrators with SMC was explored using output feedback designs as a high-gain observer for interacting and non-interacting tanks. The validation of proposed method demonstrates good tracking performance in spite of unmodeled dynamics and external disturbances (Prusty et al., 2020). Zhao et al. (2022) designed terminal SMC (TSMC) to solve the problem of signularity and mismatched uncertainty. To eliminate reaching phase of TSMC, a state transformation method was used. The numerical simulation explored the efficacy of proposed method while authors (Pourhashemi et al., 2019) presented fractional TSMC and dynamic fractional TSMC with novel sliding manifold in a simulation environment to reduce singularity problem, and increase convergence rate.

The different control techniques such as super-twisting controller (STC), optimal, global, observers, second and higher-order SMC, etc. were adopted by researchers to alleviate chattering effect. The conventional second-order SMC cannot be extensively used practically as relative degree of control signal is two or more. To solve the problem, the best option is use of STC. However, researchers have to select the gain coefficients of sliding manifold and control law very precisely. The work is complicated and frustrating. Parameter convergence is another challenging task (Laware et al., 2020).

To solve above difficulties, some of the researchers have used modern optimisation techniques, fuzzy logic, genetic algorithms, artificial neural network, etc. Some of them have used hybrid controller combinations for tuning parameters to improve overall metrics of the systems (Espin et al., 2023). PID controller-based particle swarm optimisation and teacher learning-based optimisation algorithms are explored to control concentration, and temperature of continuous stirred tank reactor. The system performance was improved by minimising mean square error and finding optimal values of PID controller parameters. The simulation tests validates the proposed strategy (Srivastava and Srivastava, 2019) while genetic algorithm and ant colony optimisers were used for tuning SMC parameters. The validation of results has been carried out for hydraulic servo system with 2-degree of freedom (Mpanza and Pedro, 2016).

In process plants such as boiler, distillation column, dairy, food, nuclear power plants, etc. precise fluid level control is the most important as the fluids are transported from tank to tank. Thus, it becomes a benchmark problem from conventional to advanced control system. It is interesting control problem due to complexities and nonlinearities. It has been attracted more researchers to process control engineering problem. There have been major developments in different control strategies for process plants with simulation studies (Govinda Kumar and Arunshankar, 2020; Mpanza and Pedro, 2016; Prusty et al., 2020; Rajesh and Deepa, 2020; Zuo et al., 2017) and real-time applications (Chawla and Singla, 2021; Kaya, 2007; Laware et al., 2022, 2023b).

Some researchers have used artificial intelligence-based strategies. An improved multi-scale edge labelling neural network under small samples has been explored to improve accuracy of tool wear condition monitoring system. The updation of tool wear condition was established via weighted voting method. The efficacy of proposed method was validated using experimental tests (Zhou et al., 2022) while Zhou et al. (2022) explored a entropy-based sparsity measure for prognosis of bearing defects and defects in axial piston pump. They reformulated divergence measure to a probabilistic entropy and validated proposed strategy to existing tools such as spectral kurtosis, protugram and fast kurtogram.

In the current work, integral dynamics with constant parameter has been added to sliding surface of typical SMC to improve steady-state accuracy and transient performance. An experimental evaluation has been carried out such that IASMC is designed to a laboratory process control system (level). The efficacy of proposed design method is validated experimentally and results are compared with prevalent control strategies.

Table 1 tabulates type of control strategy adopted by the earlier researchers, key references and the identified research gaps. In Table 1, hybrid control includes comination of PID, model predictive control and SMC with other control structures.

**Table 1** Summary of adopted control strategy, key references and research gaps

| *Control method* | *Key references* | *Research gap* |
|---|---|---|
| PID | Dalen and Ruscio (2018) | Robustness issue |
| | Joseph et al. (2022) | Global heterogeneity |
| | Jiao et al. (2021) | Steady-state error |
| | Karanam and Shaw (2022) | Stability and robustness |
| | Rajesh and Deepa (2020) | Oscillatory and slow response |
| | Zuo et al. (2017) | Stability reduction |
| Classical SMC and variants | Abdelhedi and Derbel (2019) | Steady-state accuracy |
| | Castellanos-Cardenas et al. (2022) | Chattering |
| | Camacho and Rojas (2000) | Fine-tuning of parameters |
| | Flores-Guerrero et al. (2021) | Transient accuracy |
| | Kaya (2007) | Overshoot and long settling time |
| | Laware et al. (2022) | Signularity problem |
| | Prusty et al. (2020) | Steady-state accuracy |
| | Siddiqui et al. (2020) | Chattering in control signal |
| | Seyedtabaii (2020) | Accuracy and robustness |
| | Utkin et al. (2020) | Chattering and long settling time |
| Hybrid control | Chawla and Singla (2021) | Steady-state accuracy |
| | Espin et al. (2023) | Transient accuracy |
| | Govinda Kumar and Arunshankar (2022) | Overshoot and settling time |
| | Laware et al. (2020) | Over-adjustment of parameters |
| | Lamzouri et al. (2022) | steady-state and transient accuracy |
| | Laware et al. (2023b) | Fine tuning of parameters |
| | Mpanza and Pedro (2016) | Transfer learning |
| | Pati and Negi (2019) | Searching ability |
| | Wu and Zhao (2023) | Convergence of parameters |

The practical challenges of SMC and its variants are as follows:

1 The challenge in real-time implementation is how to improve the performance of a system using 'best' parameter.

2 For steady-state and dynamic responses, how to make a trade-off is another challenge.

3 Parameter tuning is not instinctive.

The major contributions are as follows:

1 Firstly, contribution is regarded as a way to combine SMC with other controller (high level controller) that aims at stabilising the nominal plant.

2 The practicability of IASMC strategy to complex control system.

3 Most of the researchers have added integral dynamics to conventional sliding surface for motion control systems. A very few researchers have worked on process control problems. Therefore, the study validates IASMC for level control plant.

4 Using Lyapunov candidate function, stability verification of IASMC is done.

5 A comparison between classical controllers and IASMC design is presented.

Thus, the main contribution of the present study is that cited limitaions of SMC are removed with proposed controller.

To control the mechanical systems, motion control strategy is used where as process control is used for unit operations and unit processes. The variables involved in motion control problems are position, displacement, speed and acceleration while temperature, flow, level, etc. are the variables in process control problem. Examples of motion control are robotics, underwater vehicle control, direction control, etc. The chemical processes, manufacturing processes, etc. are associated with process control problem.

The structure of article is: Section 2 devises the problem formulation. Section 3 presents controller designs while laboratory experimental setup and test results are accorded in Section 4. A summary of work is presented finally.

## 2 Motivation and problem formulation

### *2.1 Motivation*

In an industrial applications for the servo and regulatory problems, zero steady-state error is desired. During reaching phase in SMC, the invariance is not guaranteed and system response is sensitive to parametric uncertainties, and bounded external disturbances (Pan et al., 2018). Hence, in this article, integral sliding-mode control design method is adopted for process (level) plant to enhance overall response of the system to eliminate 'reaching phase' and to ensure invariance from initial time instant.

### 2.2 Problem formulation

A linear perturbed second-order plant model with disturbance and uncertainty terms is as (Seyedtabaii, 2020; Chawla and Singla, 2021; Shaker, 2016)

$$\ddot{\omega}(t) = -(A + \Delta A)\dot{\omega}(t) - (B + \Delta B)\omega(t) + (C + \Delta C)u(t) + d(t) \tag{1}$$

where estimated (nominal) system parameters are shown by A, B and C. $\Delta A$, $\Delta B$ and $\Delta C$ represents uncertainty terms due to perturbations in system parameters, non-linearity and unmodeled dynamics while $d(t)$ shows internal, external and bounded disturbances, i.e., unknown perturbations. $u(t)$ is the controller output and $\omega(t)$ is controlled variable.

Without disturbances, the dynamic model of second-order plant in equation (1) can be rearranged as (Wu et al., 2022; Shome et al., 2021; Laware et al., 2023b)

$$\ddot{\omega}(t) = -A\dot{\omega}(t) - B\omega(t) + Cu(t) + U \tag{2}$$

where $U$ denotes unknown and bounded uncertainty. $|U| \leq U_{\max}$, $U_{\max} \in R^+$ ($R^+$ is a set of positive real constants). Uncertainty $U$ is given by (Kaya, 2007)

$$U = \pm\Delta A\dot{\omega}(t) \pm \Delta B\omega(t) \pm \Delta Cu(t) + d(t) \tag{3}$$

The upper-bound of uncertainty $U_{\max}$ is (Abdelhedi and Derbel, 2019; Laware et al., 2023b)

$$U_{\max} = +\Delta A|\dot{\omega}(t)| + \Delta B|\omega(t)| + \Delta C|u(t)| + |d(t)| \tag{4}$$

General tracking error $e(t)$ is (Dalen and Ruscio, 2018)

$$e(t) = r(t) - \omega(t) \tag{5}$$

where $r(t)$ is command signal.

Following are the assumptions related to equation (1) (Gambhire et al., 2021; Du et al., 2019):

*Assumption 1:* The differentiation with respect to time is possible with equations (2) and (3).

*Assumption 2:* $|d(t)| \leq U_{\max}$ [equation (4)].

## 3 Controller synthesis

The section explores design of conventional PID controller, SMC and IASMC for laboratory process (level) control system.

### 3.1 Conventional PID controller

PID controllers are widely used in industrial processes. It has three gains to be tuned. The control signal efforts of PID controller are calculated as (Jiao et al., 2021)

$$u(t) = k_p e(t) + k_i \int_0^t e(t)dt + k_d \dot{e}(t) \tag{6}$$

where $u(t)$ and $e(t)$ represents control signal, and tracking error signal respectively. $k_p$, $k_i$ and $k_d$ are PID gains of PID controller to be tuned respectively. PID controller eliminates steady-state error (due to integral gain) and output changes are anticipated with the help of derivative gain (Du et al., 2019). $t$ is period over which experimental tests have been performed. Real-time experimentation is carried out for $t$ = 1,000 sec.

### 3.2 Classical sliding mode controller

In classical SMC, sliding surface $\sigma(t)$ is represented by equation (7) such that $\sigma(t) = f(e(t), \dot{e}(t))$ (Shaker, 2016).

$$\sigma(t) = \left(\lambda + \frac{d}{dt}\right)^{n-1} e(t) \tag{7}$$

where $n$ is the order of uncontrolled system, $\lambda$ is the positive tuning constant and $\lambda \in R^+$. For $n$ = 2, the solution of equation (7) is a straight line passing through the origin. Sliding manifold acknowledges a constant value for $\dot{\sigma}(t)$ = 0 once the reference point is reached.

The two-fold expression for total control law is (Utkin et al., 2020; Siddiqui et al., 2020)

$$u(t) = u_{eq}(t) + u_{dis}(t) \tag{8}$$

In equation (8), $u(t)$ is total control input, $u_{eq}(t)$ is equivalent control law while $u_{dis}(t)$ is discontinuous control signal and given by (Govinda Kumar and Arunshankar, 2022)

$$u_{dis}(t) = k_d sgn(\sigma(t)) \tag{9}$$

Equation (9) is with 'sgn' function and it is responsible for 'chattering'. For alleviating chattering, many researchers have used 'sigmoid' function as $u_{dis}(t) = k_d(\sigma(t))/[abs(\sigma(t)] + \delta)]$ in which $k_d$ is the discontinuous gain and $\delta$ is boundary-layer thickness. Further, to reduce chattering, tangential hyperbolic function is used as (Laware et al., 2022)

$$u_{dis}(t) = k_d(tanh)\frac{\sigma(t)}{\beta} \tag{10}$$

### 3.3 Integral augmented sliding mode controller

To improve steady-state error and transient behaviour, an integral term has been added to equation (7) as (Pan et al., 2018; Shaker, 2016; Samira and Renuganth, 2017)

$$\sigma(t) = \left(\lambda + \frac{d}{dt}\right)^{n-1} e(t) + K_i \int_0^t e(t)dt \tag{11}$$

In equation (11), $K_i \in R^+$ is an integral constant. Equation (11) denotes three-dimensional plane in which solutions are on a plane passing through the origin for $n$ = 2. For conventional SMC, solutions are on a line.

### *3.4 Verification of stability*

The total control law in equation (8) must be designed such that tracking error tends to zero. In sliding phase, $\sigma(t) = \dot{\sigma}(t)$ = 0 and $u_{eq}(t)$ is determined. In reaching phase, $\sigma(t) \neq 0$ and $u_{dis}(t)$ has been formulated (Siddiqui et al., 2020). For $n$ = 2, with respect to time, derivative of equation (11) gives,

$$\dot{\sigma}(t) = \lambda\dot{e}(t) + \ddot{e}(t) + K_i e(t) \tag{12}$$

$\dot{\sigma}(t)$ = 0 is a necessary condition for tracking error $e(t)$ to present and remains on sliding manifold (Shome et al., 2021). Therefore, from equation (12)

$$\lambda\dot{e}(t) + \ddot{e}(t) + K_i e(t) = 0 \tag{13}$$

If gain coefficients in equation (13) are properly selected then equation (13) is strictly stable, i.e., $\lim_{t\to\infty} e(t)$ = 0 which indicates that feedback system is asymptotically stable (Govinda Kumar and Arunshankar, 2018; Camacho and Rojas, 2000).

Substituting double-derivative of equation (5) and estimated parameters of process system into equation (12), yielding,

$$\dot{\sigma}(t) = \lambda\dot{e}(t) + K_i e(t) + \ddot{r}(t) + A\dot{\omega}(t) + B\omega(t) - Cu(t) - d(t) \tag{14}$$

with unknown lumped uncertainty $d(t)$ = 0 and $\dot{\sigma}(t)$ = 0, one has an equivalent control signal $u_{eq}(t)$ as (Samira and Renuganth, 2017)

$$u_{eq}(t) = \frac{1}{C}[\lambda\dot{e}(t) + K_i e(t) + \ddot{r}(t) + A\dot{\omega}(t) + B\omega(t)] \tag{15}$$

Consider a Lyapunov candidate function to deduce the reachability condition as (Laware et al., 2023a)

$$V(t) = \frac{1}{2}\sigma^2(t) \tag{16}$$

with $V(0)$ bounded and $V(t)$ is non-increasing, for all $\sigma(t) \neq$ 0. Derivative of equation (16) is,

$$\dot{V}(t) = \sigma(t)\dot{\sigma(t)} < 0, \sigma(t) \neq 0 \tag{17}$$

Further, inserting the system variables and constants into equation (17), yielding

$$\begin{aligned}\sigma(t)\dot{\sigma}(t) = \sigma(t)[&\ddot{r}(t) + A\dot{\omega}(t) + B\omega(t) \\ &- C(u_{eq}(t) + u_{dis}(t)) + \lambda e(t) + K_i e(t)]\end{aligned} \tag{18}$$

Considering the disturbance term $d(t)$ and substituting equation (15), and equation (9) into equation (18), it is obtained as,

$$\dot{\sigma}(t) = -k_d sgn(\sigma(t)) - d(t) \tag{19}$$

substituting equations (19) into (17), yielding,

$$\begin{aligned}\dot{V}(t) &= \sigma(t)[-k_d C sgn(\sigma(t)) - d(t)] \\ &= -k_d C|\sigma(t)| - \sigma(t)d(t) \\ &\leq k_d C|\sigma(t)| + |\sigma(t)||d(t)| \\ &\leq -|\sigma(t)|[k_d C - U_{\max}]\end{aligned} \tag{20}$$

Equation (20) is a negative semi-definite function and $\sigma(t)$ converges to zero in a finite-time and stability conditions are:

1 $\sigma(t)\dot{\sigma}(t) < 0$

2 $k_d C > U_{\max}$.

The total control law for implementation with equation (10) is,

$$u(t) = \frac{1}{C}[\ddot{r}(t) + A\dot{\omega}(t) + B\omega(t) + \lambda\dot{e}(t) + K_i e(t)] + k_d(tanh)\frac{\sigma(t)}{\beta} \tag{21}$$

In equation (21), $A$, $B$, $C$ devises nominal system parameters which are determined at equilibrium point of the system, $\lambda$ is the tuning parameter responsible for convergence of sliding surface, $e(t)$ is the tracking error, $K_i$ is integral gain coefficient that determines the amount of steady-state error, $k_d$ is switching gain in tangential hyperbolic function and $\beta$ shows the boundary layer thickness responsible for chattering.

## 4 Real-time experimentation

The section explores real-time experimental results for nominal system parameters, reference-point tracking and bounded disturbance rejection tests.

### *4.1 Nominal response*

For the demonstration of real-time applicability of IASMC, conventional SMC and PID controller, a laboratory level plant is shown in Figure 1. An experimental setup facilitates a tank with hand valve at bottom side for fluid flow discharge to basin.

Inflow-rate ($Q_{in}$) to the tank varies with 230 V, 50 $H_z$ motor which drives the pump. At equilibrium condition, $Q_{in}$ and outflow-rate ($Q_{out}$) are same. A personal computer (Pentium IV, 300 $MH_z$, 256 RAM) is used for experimental tests. The controlled variable (level) is measured from level transmitter which provides 4–20 mA DC signal corresponding to 0–100% output level. Table 2 summarises specifications of the system under consideration.

Figure 2 shows a schematic diagram for controller realisation. The process system is interfaced to computer via a data acquisition card PCI6024E and BNC connector 2120. A 4–20 mA DC signal from level sensor is applied to analogue input of BNC 2120 connector through electronics current-voltage converter circuit. Controller signal (0–5 V) is applied to analogue output of BNC 2120 connector and converted to a current signal of 4–20 mA DC. The signal is applied as input signal to a variable frequency drive (VFD) which drives pump varying inflow-rate to the tank. For experimental tests, algorithm is developed in MathWorks MATLAB/SIMULINK2009a.

**Figure 1** Real-time experimental setup (see online version for colours)

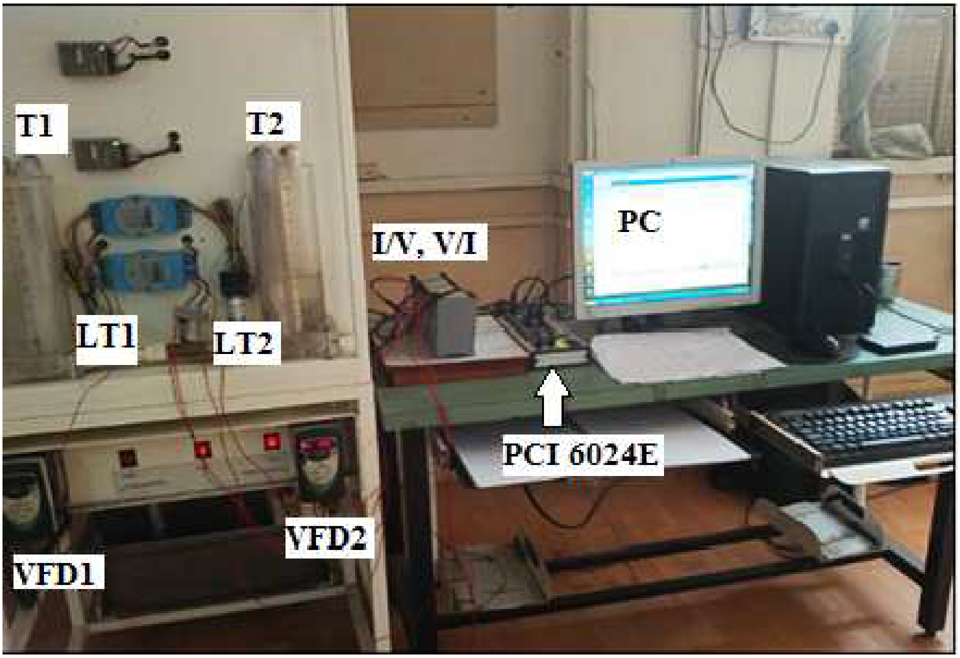


*Source:* Laware et al. (2020)

**Table 2** Parameters of experimental setup

| *Setup parameters* | *Particulars* |
|---|---|
| Tank height | 26.5 cm, 0–100% scale |
| Tank area | 66.4 $cm^2$ |
| Variable frequency drive | 4–20 mA DC input and 230 V AC output |
| Sensor sensitivity | 0.604 mA/cm |
| Actuator sensitivity | 0.17 $cm^3$/sec./V |
| $Q_{in}$ at equilibrium | 39.4 $cm^3$/sec. |
| $Q_{out}$ at equilibrium | 39.0 $cm^3$/sec. |

The discontinuous signal $u_{dis}(t)$ and equivalent signal $u_{eq}(t)$ is sent to level control system through PCI6024E DAQ card. Initially, the level system is tested to obtain nominal parameter coefficients $A$, $B$ and $C$. Without closed-loop operation, an equivalent control law has been deduced. In manual mode, a step signal of 2.5 V amplitude (50% output level) is forcing input to level control plant. Real-time system has been modeled as first-order plus dead-time model.

Figure 3 depicts the performance of actual and approximated response of a plant. In Figure 3, solid blue line denotes output of real plant whereas dotted red line represents approximated response. The controlled variable (level) settles down after 100 sec. and error is ±2.1%. Therefore, modelling error in an approximated system is ±2.1/40 = ±0.0526%. This implies that open-loop response of approximated and actual plant matches to each other. The validation of same is carried out for 17% level.

**Figure 2** Controller realisation: a schematic diagram

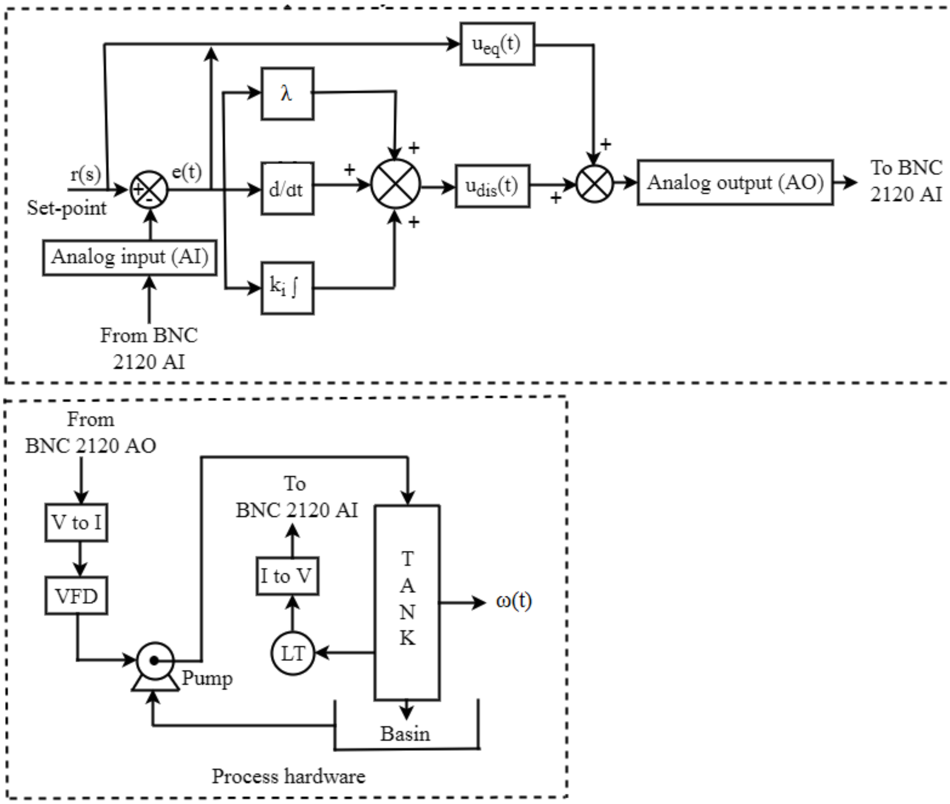


The modelling of level plant is based on process reaction curve (PRC) method. The general expression of transfer function in PRC method is (Dalen and Ruscio, 2018)

$$G_p(s) = \frac{K_p}{\tau_p s + 1} e^{-\theta s} \tag{22}$$

where $K_p$ is static gain, $\tau_p$ is time-constant and $\theta$ is dead-time of level plant.

Therefore, transfer function of the plant in first-order with dead-time form is,

$$G_p(s) = \frac{0.785}{41.32s + 1} e^{-4.12s} \tag{23}$$

In equation (23), static gain, $K_p$ = 0.785, process time-constant, $\tau_p$ = 41.32 sec. and dead-time, $\theta$ = 4.12 sec. The approximated plant model of equation (23) is (Castellanos-Cardenas et al., 2022),

$$G_p(s) = \frac{0.004611}{s^2 + 0.267s + 0.005874} \tag{24}$$

From equation (24), the estimated (nominal) plant parameters are to be: $A$ = 0.267, $B$ = 0.005874 and $C$ = 0.004611.

**Figure 3** Open-loop response of actual and approximated model (see online version for colours)

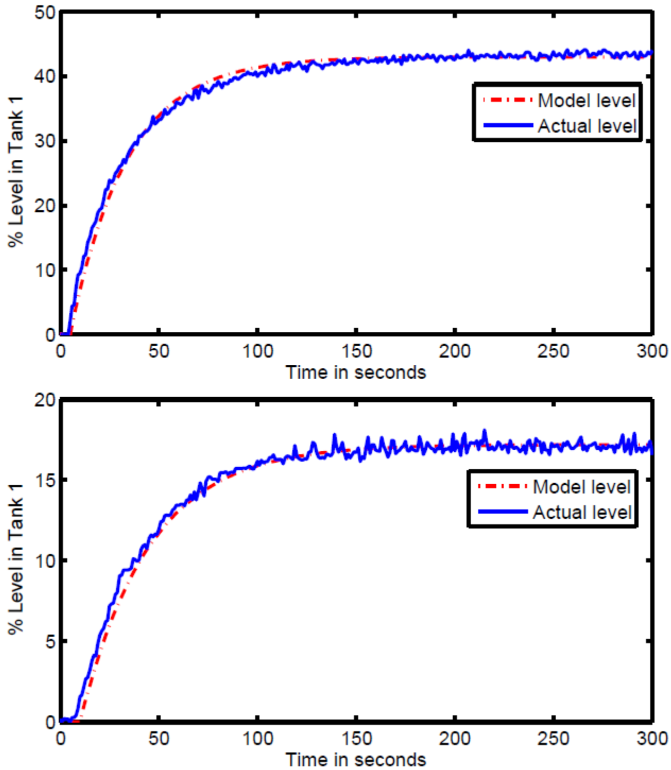


The total control law presented by equation (21) is implemented for approximated plant shown by equation (24) with proper selection of controller parameters. The proposed design method (IASMC) is compared to SMC reported by Kaya (2007) and Camacho and Rojas (2000). To choose SMC parameters, the tuning equations in Kaya (2007) and Camacho and Rojas (2000) were used while intuitive judgement is used to find the controller parameters of IASMC and PID control strategies based on following guidelines (Camacho and Rojas, 2000; Samira and Renuganth, 2017; Govinda Kumar and Arunshankar, 2022)

1 equation (13) must be stable

2 SMC parameters $\in R^+$

3 non-overshoot response is desired

4 chattering efforts must be minimum or no chattering should be there.

Based on these guidelines, authors have selected the controller parameters. The heuristic method is used for determination of controller parameters. Table 3 provide summary of selected parameters for the reported algorithms.

The closed-loop performance for 0–40% level step change has been illustrated in Figures 4(a) and 4(b) for reported control design strategies. As seen from Figure 4(a), the control performance of IASMC is better than Kaya (2007), Camacho and Rojas (2000) and PID controller as non-overshoot response, smaller rise time, settling time, reaching time (rise time + delay in output), delay-time in output and deviation in steady-state response were obtained with proposed control strategy. Besides, prevalent design methods show overshoots, large settling time in magnitude.

**Table 3** Parameter selection for reported strategies

| *Control strategy* | *Parameters of $\sigma(t)$/ gain coefficients* | *Parameters of $u_{dis}(t)$* |
|---|---|---|
| IASMC | $\lambda = 0.3,\ K_i = 0.565$ | $k_d = 3.5,\ \beta = 0.15$ |
| Kaya (2007) | $k_1 = 0.2669,\ k_2 = 0.0178$ | $k_d = 5.767$ |
| | $k_3 = 0.1334,\ k_4 = 1.5$ | $\Omega = 1.24$ |
| Camacho and Rojas (2000) | $\lambda_0 = 0.0178,\ \lambda_1 = 0.2669$ | $k_d = 5.767,\ \delta = 0.825$ |
| PID controller | $k_p = 1.26,\ k_i = 0.08$ and $k_d = 0.00021$ | Not applicable |

**Figure 4** Controlled variable response of IASMC, Kaya (2007), Camacho and Rojas (2000) and PID controller, (a) nominal output to 0–40% step set-point level change (b) associated control efforts (see online version for colours)

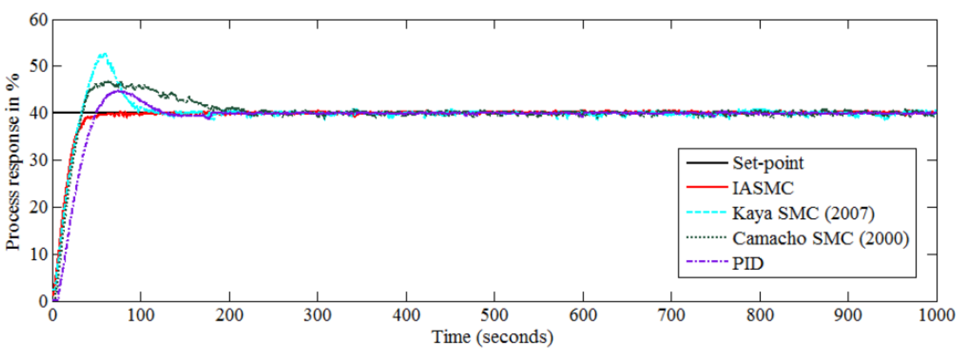


(a)

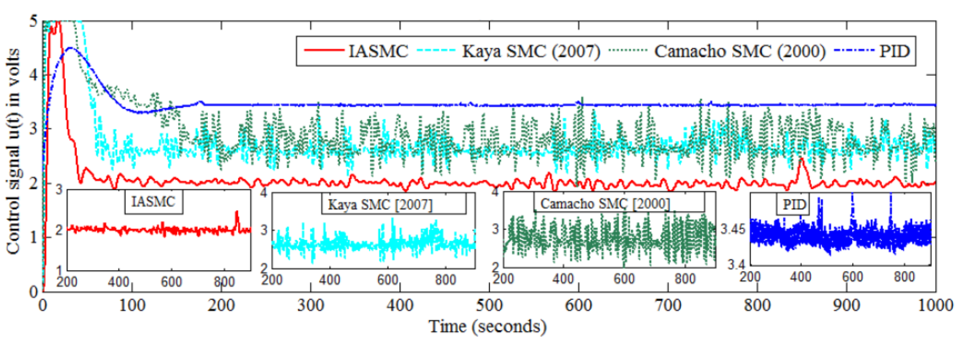


(b)

The control signal trends are shown in Figure 4(b). In the transient state, control efforts are more while it is smaller in steady-state conditions. The control signal settles down in 44.6 sec., 67.1 sec., 164.1 sec. and 185.4 sec. for IASMC, Kaya (2007), Camacho and Rojas (2000), and PID control respectively. As seen from magnifier at bottom side in Figure 4(b), the controller output variations for Kaya (2007), Camacho and Rojas (2000), and PID control design are large in magnitude.

Tables 4 and 5 illustrates quantitative performance indicators evaluated from Figure 4(a) as time-domain specifications and error-based performance indices which show the superiority of proposed technique. As seen from Table 5, for IASMC method, the error-based performance indices (shows quality of controlled response) have better controlled response (minimum values) than other design methods.

**Table 4** Time-domain specifications

| *Control method* | *Rise time sec.* | *Settling time sec.* | *Overshoot in %* | *Output deviation %* | *Reaching time sec.* | *Output delay sec.* |
|---|---|---|---|---|---|---|
| IASMC | 17.5 | 51.2 | 0 | ± 1.08 | 19.7 | 2.2 |
| Kaya (2007) | 18.6 | 105.9 | 12.83 | ± 1.95 | 22.4 | 3.8 |
| Camacho and Rojas (2000) | 20.3 | 184.6 | 6.97 | ± 1.46 | 24.6 | 4.3 |
| PID | 29.02 | 120.1 | 4.82 | ± 1.37 | 35.92 | 6.9 |

**Table 5** Error-based performance indices

| *Control method* | *IAE* | *ISE* | $P_1$ | $P_2$ | $P_3$ |
|---|---|---|---|---|---|
| IASMC | 37.51 | 15.71 | 13.24 | 573.50 | 586.73 |
| Kaya (2007) | 38.33 | 20.74 | 11.81 | 637.70 | 649.51 |
| Camacho and Rojas (2000) | 48.28 | 23.33 | 14. 32 | 833.85 | 848.17 |
| PID | 40.41 | 30.31 | 14.14 | 1,024 | 1,039 |

Tables 6 and 7 illustrates percent improvement of IASMC strategy over other reported control methods in terms of time domain mertics and error-based indices. However, from Table 7, it is investigated that Kaya (2007) has an improvement of 12.1% over IASMC technique for equation (27).

Following error-based performance indices are used.

$$IAE = \int_0^t |e(t)|dt \tag{25}$$

$$ISE = \int_0^t [e(t)^2]dt \tag{26}$$

$$P_1 = \int_0^t [p_1 IAE + p_2 ISE]dt \tag{27}$$

$$P_2 = \int_0^t [p_3(e(t)^2) + p_4(u(t)^2)]dt \tag{28}$$

$$P_3 = \sum_{i=1}^{2} (P_1 + P_2) \tag{29}$$

In equations (27) and (28), the equivalent weights are selected as: $p_1$ = 0.6, $p_2$ = 0.4, $p_3$ = 0.9 and $p_4$ = 0.1 (Laware et al., 2020).

**Table 6** An accuracy level (%) of IASMC method in time-domain specifications over reported methods

| *Control method* | *Rise time (%)* | *Settling time (%)* | *Overshoot in (%)* | *Deviation in (%)* | *Reaching time (%)* | *Output delay (%)* |
|---|---|---|---|---|---|---|
| Kaya (2007) | 51.65 | 5.91 | 100 | 44.62 | 12.05 | 42.11 |
| Camacho and Rojas (2000) | 72.3 | 13.8 | 100 | 26.02 | 19.92 | 48.84 |
| PID | 57.4 | 39.7 | 100 | 21.16 | 45.2 | 68.16 |

**Table 7** An accuracy level (%) of IASMC in error-based performance indices over reported methods (see online version for colours)

| *Control method* | *IAE (%)* | *ISE (%)* | $P_1$ *(%)* | $P_2$ *(%)* | $P_3$ *(%)* |
|---|---|---|---|---|---|
| Kaya (2007) | 2.15 | 24.35 | –12.1 | 10.07 | 9.67 |
| Camacho and Rojas (2000) | 22.31 | 32.73 | 7.55 | 31.22 | 30.82 |
| PID | 7.12 | 48.24 | 6.36 | 43.19 | 43.53 |

Figures 5(a) and 5(b) illustrate the variations of equivalent control signal $u_{eq}(t)$ and discontinuous control input $u_{dis}(t)$ for IASMC, Kaya (2007) and Camacho and Rojas (2000) respectively. It has been observed that the variations of IASMC is smaller than other SMC techniques for both equivalent control and discontinuous control in magnitude.

Figures 6(a) and 6(b) explore the trends of error $e(t)$ and sliding manifold $\sigma(t)$ during the application of control signal $u(t)$ for control law represented by equation (21). One can seen that when $\sigma(t) \neq 0$, error $e(t) \neq 0$. Sliding mode is in reaching phase at 27.8 sec., 58.6 sec. and 179.4 sec. for IASMC, Kaya (2007) and Camacho and Rojas (2000) respectively. However, from Figure 6(b), it is observed that sliding surfaces $\sigma(t)$ of Kaya (2007) and Camacho and Rojas (2000) are not exactly reaches to zero rather are at 0.03006 V and –0.1 V in this practical application. This is due to unmodeled dynamics, parametric uncertainties and bounded external disturbances. However, the average value of variable is zero.

## *4.2 Robustness analysis*

To test the robustness of controller, plant parameters in equation (23) are changed as:

1 no change has been made in the static gain of plant

2 delay-time is increased by 15%

3 process time-constant is reduced by 15%.

**Figure 5** Performance of IASMC, Kaya (2007) and Camacho and Rojas (2000), (a) an equivalent control signal $u_{eq}(t)$ (b) discontinuous control input $u_{dis}(t)$ (see online version for colours)

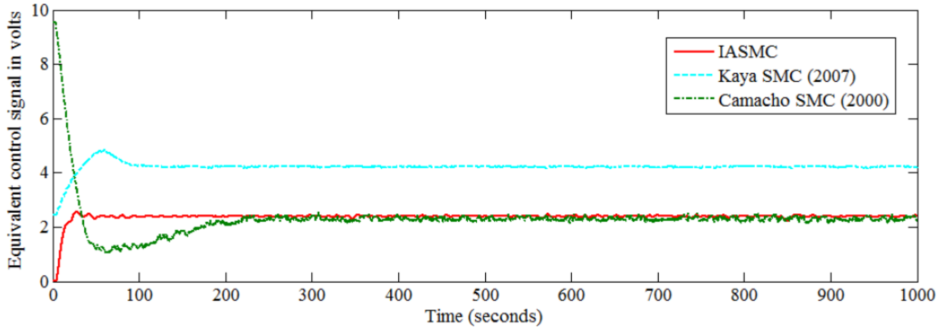


(a)

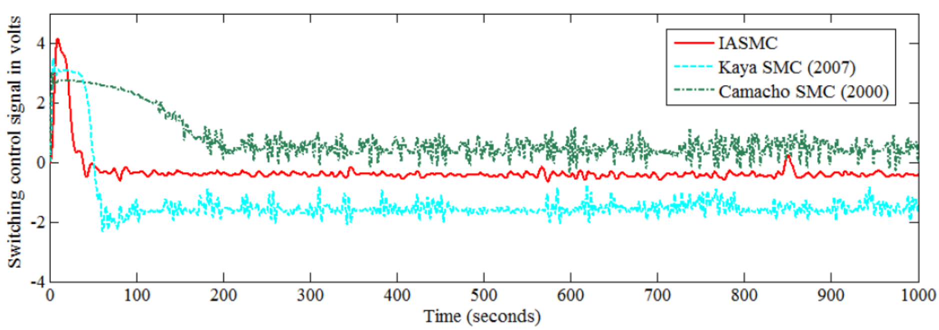


(b)

Therefore, 15% uncertainty has been introduced in the plant model. For the following plant represented by equation (30), a set-point change and disturbance rejection tests have been conducted.

$$G_p(s) = 0.785\frac{e^{-4.738s}}{(35.122s + 1)} \tag{30}$$

The performance for reference-point level change and disturbance has been illustrated in Figure 7(a) while controller efforts are depicted in Figure 7(b). In Figure 7(a), reference-point is changed from 40% to 50% for the period of 250 sec. to 750 sec. and back to 40% from 750 sec. A disturbance of 12% magnitude is applied at 500 sec. and 900 sec. for the period of 10 sec. duration. It is observed that command tracking and disturbance rejection of IASMC strategy is better than other design techniques.

As seen from Figure 7(b), initially, in transient condition, the control efforts are large while variations are less for IASMC in a steady-state response. Control signal variations are more for Kaya (2007), Camacho and Rojas (2000) and PID controller.

The typical performances such as tracking error $e(t)$, sliding surface $\sigma(t)$, equivalent control input $u_{eq}(t)$ and discontinuous control input $u_{dis}(t)$ under uncertainties and external bounded disturbances are depicted in Figures 8(a), 8(b), 8(c) and 8(d). From Figures 8(a) and 8(b), it is seen that tracking error and sliding surface converges at zero fastly for the proposed strategy than other methods while from Figures 8(c) and 8(d) it is observed that IASMC explores smaller variations in both the control laws than reported control techniques. Thus, command tracking and disturbance rejection/suppression capability of IASMC is better than Kaya (2007), Camacho and Rojas (2000), and PID controller.

**Figure 6** Typical performance, (a) tracking signal $e(t)$ of IASMC, Kaya (2007), Camacho and Rojas (2000) and PID controller (b) sliding signal $\sigma(t)$ of IASMC, Kaya (2007) and Camacho and Rojas (2000) (see online version for colours)

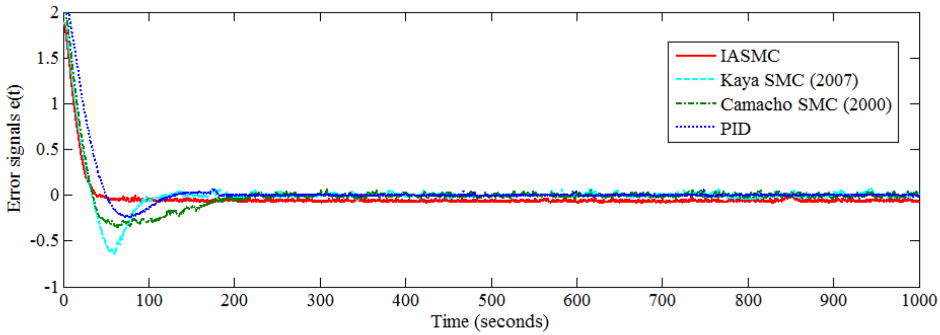


(a)

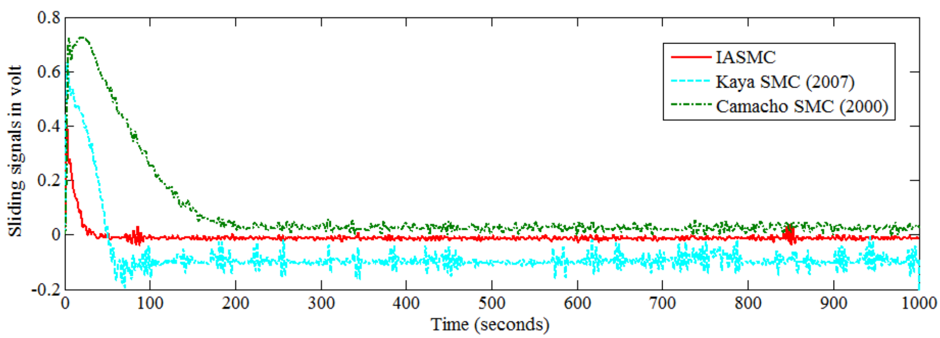


(b)

**Figure 7** Control performance of IASMC, Kaya (2007), Camacho and Rojas (2000) and PID controller, (a) set-point tracking and disturbance rejection with 15% uncertainty (b) associated controller output $u(t)$ (see online version for colours)

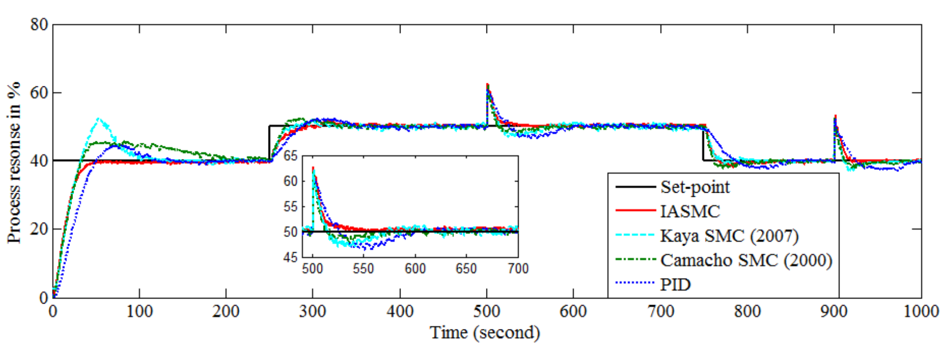


(a)

**Figure 7** Control performance of IASMC, Kaya (2007), Camacho and Rojas (2000) and PID controller, (a) set-point tracking and disturbance rejection with 15% uncertainty (b) associated controller output $u(t)$ (continued) (see online version for colours)

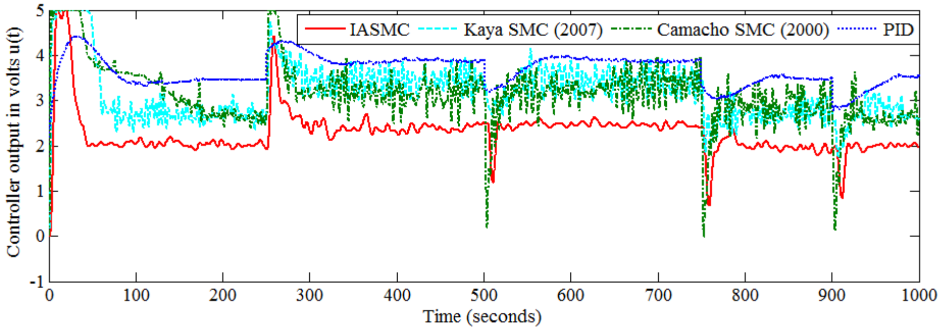


(b)

**Figure 8** Typical performance, (a) tracking error $e(t)$ (b) sliding signal $\sigma(t)$ (c) an equivalent control input $u_{eq}(t)$ (d) discontinuous control input $u_{dis}(t)$ of IASMC, Kaya (2007) and Camacho and Rojas (2000)

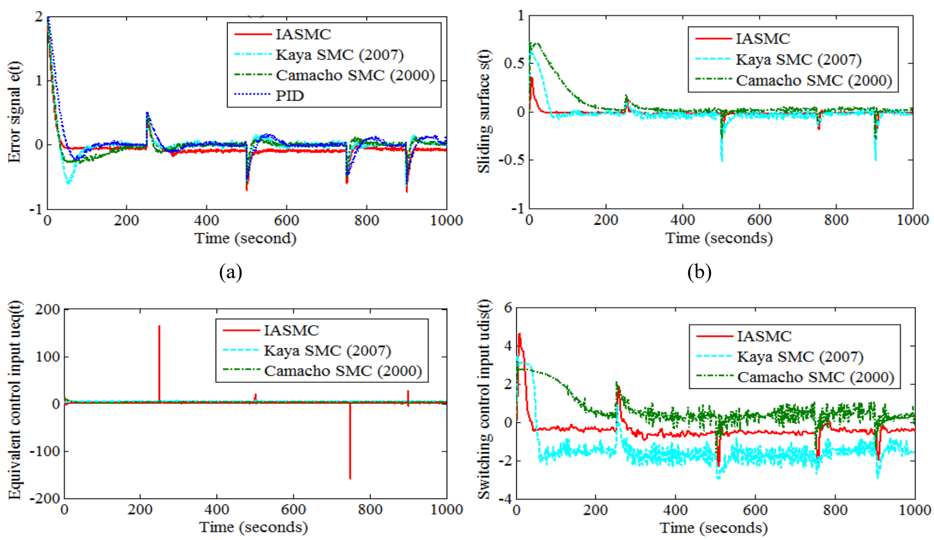


(a) (b) (c) (d)

## 5 Conclusion

An IASMC is proposed to enhance overall output response of process plant with the assumption that nominal plant dynamics are known. IASMC technique is used to control the level. An approximate model from first-order with dead-time is used and validated experimentally. Effectiveness of the proposed method is verified for nominal (estimated) plant parameters, step signal set-point change and applied disturbances. To alleviate chattering effect, a hyperbolic tangential function is used. The stability analysis is presented using a Lyapunov candidate function.

From the experimental results, time domain and error-based metrics depicted in Tables 4, 5, 6 and 7, it can be concluded that performance of IASMC has been significantly improved over Kaya (2007), Camacho and Rojas (2000), and conventional PID controller. Table 5 explores the better controlled response for the proposed strategy than other techniques. Therefore, one can think IASMC as a alternative controllers in industrial applications as it provides non-overshoot response, smaller settling time, rise time, reaching time, delay-time in output and less deviations in steady-state response. Thus, comprehensive experimentation demonstrates the arguments of study and have demonstrated superior performance in terms of chattering attenuation, tracking error and disturbance rejection.

Experimental result reveals the merits for augmentation of integral dynamics to sliding surface $\sigma(t)$. The advantages of proposed design technique are:

1 control calculations and design is easy

2 easy tuning as guidelines and tuning equations are available

3 experimental model-based designs are not complex as compared to theoretical ones

4 the mathematical expression of sliding surfce is concise and easy for implementation.

The graphical and statistical results validates the advantages of proposed strategy.

Performance of IASMC gets degrade with the modifications in integral sliding dynamics. It is observed that IASMC belongs to a kind of global SMC. In the future direction of work, an optimisation algorithms can be embedded to explore the optimum parameters of the proposed controller. The applicability of suggested control design method to handle perturbations in composite learning control would be interesting for future study.

## References

Abdelhedi, F. and Derbel, N. (2019) 'On the renovation and analysis of higher-order sliding mode approaches with application to robotic systems', *International Journal of Modelling, Identification and Control*, Vol. 31, No. 4, pp.374–381 https://doi.org/10.1504/IJMIC.2019.099830.

Camacho, O. and Rojas, R. (2000) 'A general sliding mode controller for nonlinear chemical processes', *Journal of Dynamic Systems, Measurement and Control, Transactions of ASME*, Vol. 122, pp.650–655 https://doi.org/10.1115/1.1318351.

Castellanos-Cardenas, D., Castrillon, F., Vasquez, R.E., Posada, N.L. and Camacho, O. (2022) 'A new sliding mode control tuning approach for second-order inverse-response plus variable dead-time processes', *Journal of Process Control*, Vol. 115, pp.77–88 https://doi.org/10.1016/j.jprocont.2022.05.001.

Chawla, I. and Singla, A. (2021) 'Real-time stabilization control of rotary inverted pendulum using LQR-based sliding mode controller', *Arab Journal of Science and Engineering*, Vol. 46, pp.2589–2596 https://doi.org/10.1007/s13369-020-05161-7.

Dalen, C. and Ruscio, D.D. (2018) 'A novel process-reaction curve method for tuning PID controllers', *Modeling, Identification and Control*, Vol. 39, No. 4, pp.273–291 https://doi.org/10.4173/mic.2018.4.4.

De Maity, R.R., Mudi, R.K. and Dey, C. (2022) 'Stable optimal self-tuning interval type-2 fuzzy controller for servo position control system', *International Journal of Automation and Control*, Vol. 16, No. 5, pp.594–620 https://doi.org/10.1504/IJACC.2022.10048165.

Du, H., Hu, X. and Ma, C. (2019) 'Non-overshooting control of linear system by a simple asymptotic gain scheduling method', *Transactions of the Institute of Measurement and Control*, Vol. 41, No. 15, pp.4187–4196 https://doi.org/10.1177/0142331219851914.

Espin, J., Estrada, S., Benitz, D. and Camacho O. (2023) 'A hybrid sliding mode controller approach for level control in the nuclear power plant steam generators', *Alexandria Engineering Journal*, Vol. 64, pp.627–644 https://doi.org/10.1016/j.aej.2022.08.046.

Flores-Guerrero, A.J., De-Leon-Morates, J. and Gutierrez-Martinez, S.V. (2021) 'Advanced control design based on sliding modes techniques for power extraction maximization in variable speed wing turbine', *Renewable Energy Systems: Modelling, Optimization and Control, Advances in Nonlinear Dynamics and Chos (ANDC)*, pp.15–39.

Gambhire, S., Kishore, D.R., Londhe, P. and Pawar, S.N. (2021) 'Review of sliding mode based control techniques for control system applications', *International Journal of Dynamics and Control*, Vol. 9, No. 2, pp.363–378 https://doi.org/10.1007/s40435-020-00638-7.

Govinda Kumar, E. and Arunshankar, J. (2022) 'Control of negative gain nonlinear processes using sliding mode controllers with modified Nelder-Mead tuning equations', *Chemical Product and Process Modeling*, Vol. 17, No. 5, pp.425–438 https://doi.org/10.1515/cppm-2020-0092.

Jiao, K., Wang, B., Du, Q., Wang, Y., Zhang, G., Yang, Z., Deng, H. and Xie, X. (2021) 'Water and thermal management of proton exchange membrane fuel cells', *Water and Thermal Management*, pp.265–314 https://doi.org/10.1016/978-0-323-91116-0.00007-9.

Joseph, S.B., Dada, E.G., Abidemi, A., Oyewola, D.O. and Khammas, B.M. (2022) 'Metaheuristic algorithms for PID controller parameters tuning: review, approaches and open problems', *Heliyons*, Vol. 11/8, No. 5, p.e09399 https://doi.org/10.1016/j.heliyon.2022.e09399.

Karanam, A.N. and Shaw, B.A. (2022) 'New two-degree of freedom combined PID controller for automatic generation control of a wind integrated interconnected power system', *Protection and Control of Modern Power Systems*, Vol. 7, No. 20, pp.1–16 https://doi.org/10.1186/s41601-022-00241-2.

Kaya, I. (2007) 'Sliding mode control of stable processes', *Industrial and Engineering Chemistry Research*, Vol. 46, pp.571–578 https://doi.org/10.1021/ie0607806.

Lamzouri, F.E., Boufounas, M. and Amrani, A. (2022) 'Power control of a stand-alone electric generation hybrid system using integral sliding mode controller', *International Journal of Automation and Control*, Vol. 16, Nos. 3/4, pp.388–409 https://doi.org/10.1504/IJACC.2022.10046273.

Laware, A.R., Talange, D.B. and Bandal, V.S. (2020) 'Experimental realization of constrained optimization of sliding mode controller parameters with modified objective functions', *International Journal of Software Computing and Testing*, Vol. 6, No. 1, pp.8–25 https://doi.org/10.37628/ijosct.v6il.594.

Laware, A.R., Awaze, S.K., Bandal, V.S. and Talange, D.B. (2022) 'The experimental validation of non-singular terminal sliding mode control for process control system', *The ECTI Transactions on Electrical Engineering, Electronics and Communications*, in press.

Laware, A.R., Patil, A.K., Bandal, V.S. and Talange, D.B. (2023a) 'Design and experimental evaluation of global sliding mode controller', *International Journal of Systems, Control and Communications*, Vol. 14, No. 1, pp.40–59 https://doi.org/10.1504/IJSCC.2022.10048704.

Laware, A.R., Navthar, R.R., Bandal, V.S. and Talange, D.B. (2023b) 'Global optimization of second-order sliding mode controller parameters using a new sliding surface: an experimental verification to process control system', *ISA Transactions*, Vol. 126, pp.498–512 https://doi.org/10.1016/j.isatra.2021.08.013.

Mat-Noh, M., Mohd-Mokhtar, R., Arshad, M.R. and Khan, Q. (2019) 'Review of sliding mode control applications in autonomous underwater vehicles', *Indian Journal of Geo Marine Sciences*, Vol. 48, No. 7, pp.973–984.

Mpanza, L.J. and Pedro, J. O. (2016) 'Sliding mode control parameter tuning using ant colony optimization for a 2-DOF hydraulic servo system', in *2016 IEEE Conf. on Automatic Control and Intelligent Systems (I2CAC15)*, pp.242–247 https://doi.org/10.1109/i2cais.2016.7885322.

Pan, Y., Yang, C., Pan, L. and Yu, H. (2018) 'Integral sliding mode control: performance, modification and improvement', *IEEE Transactions on Industrial Informatics*, Vol. 14, No. 7, pp.3087–3096 https://doi.org/10.1109/TII.2017.2761389.

Pati, A. and Negi, R. (2019) 'An optimized 2-DoF IMC-PID-based control scheme for real-time magnetic levitation system', *International Journal of Automation and Control*, Vol. 13, No. 4, pp.413–439 https://doi.org/10.1504/IJACC.2019.10020238.

Pilla, R., Gorripotu, T.S. and Karlapudy, A.M. (2021) 'Design and implementation of non-linear controller and observer for inverter fed permanent magnet synchronous motor drive using dSPACE DS1103 controller board', *International Journal of Automation and Control*, Vol. 15, No. 1, pp.78–98 https://doi.org/10.1504/IJACC.2021.10033308.

Pourhashemi, A., Ramezani, A. and Siahi, M. (2019) 'Designing dynamic fractional terminal sliding mode controller for a class of nonlinear system with uncertainties', *International Journal of Automation and Control*, Vol. 13, No. 2, pp.197–225 https://doi.org/10.1504/IJACC.2019.10010935.

Prusty, S.B., Seshagiri, S., Pati, U.C. and Mahaptra, K.K.(2020) 'Sliding mode control of coupled tank system using conditional integrators', *IEEE/CAA Journal of Automation Sinica*, Vol. 7, No. 1, pp.118–125 https://doi.org/10.1109/JAS.2019.1911831.

Rajesh, R. and Deepa, S.N. (2020) 'Design of direct MRAC augmented with 2 DoF PIDD controller: an application to speed control of a servo plant', *Journal of King Saud University-Engineering Sciences*, Vol. 32, No. 5, pp.310–320 https://doi.org/10.1016/j.jksues.2019.02.005.

Samira, E. and Renuganth, V. (2017) 'Singularity-free integral-augmented sliding mode control for combined energy and attitude control system', *Advances in Space Research*, Vol. 59, No. 2, pp.631–644 https://doi.org/10.1016/j.asr.2016.10.007.

Seyedtabaii, S. (2020) 'Modified adaptive second-order sliding mode control: perturbed system response robustness', *Computers and Electrical Engineering*, Vol. 81, p.106536 https://doi.org/10.1016/jcompeleceng.106536.

Shaker, M.S. (2016) 'Integral sliding mode approach to robust control systems against friction force', *Arab Journal of Science and Engineering*, Vol. 41, pp.3695–3702 https://doi.org/10.1007/s13369-015-1913-5.

Sharma, J. and Pratap, B. (2020) 'Robust controller design for nonlinear twin rotor control system using quantitative feedback theory', *International Journal of Automation and Control*, Vol. 14, No. 3, pp.355–376.

Shome, S.K., Jana, S., Mukherjee, A. and Bhattacharjee, P. (2021) 'Model-based control of second-order piezo actuator system with hysteresis in time-delay environment', *Turkish Journal of Electrical Engineering and Computer Science*, Vol. 29, pp.1495–1508 https://doi.org/10.3906/elk-1907-28.

Siddiqui, M.A., Anwar, M.N. and Laskar, S.H. (2020) 'Sliding mode controller design for second-order unstable processes with dead-time', *Journal of Electrical Engineering*, Vol. 71, pp.237–245 https://doi.org/ 10.1007/s11771-021-4837-0.

Srivastava, V. and Srivastava, S. (2019) 'Control of continuous stirred tank reactor (CSTR) using nature inspired algorithm', *Journal of Information and Optimization Sciences*, Vol. 40, No. 2, pp.329–338 https://doi.org/10.1080/02522667.2019.1578092.

Toshani, H. and Farrokhi, M. (2017) 'Optimal sliding-mode control of linear systems with uncertainties and input saturation using projection neural network', *Optimal Control Applications and Methods*, pp.1–18 https://doi.org/10.1002/oca.2385.

Utkin, V., Yuryorlow, P.A. and Polyakov, A. (2020) 'Conventional and higher-order sliding mode control', *Journal of the Franklin Institute*, Vol. 357, pp.10244–10261.

Wu, R. and Zhao, D. (2023) 'Lyapunov-based MPC for nonlinear process with online triggered linearised model', *International Journal of Automation and Control*, Vol. 17, No. 1, pp.1–18 https://doi.org/10.1504/IJACC.2023.10046543.

Wu, L., Liu, J., Vazquez, S. and Mazumder, S.K. (2022) 'Sliding mode control in power converters and drives: a review', *IEEE/CAA Journal of Automatica Sinica*, Vol. 9, No. 3, pp.392–406 https://doi.org/10.1109/JAS.2021.1004380.

Zhao, N., Zhang, Ye., Yang, X. and Zhao, D. (2022) 'Non-singular terminal sliding mode control for a class of second-order systems with mismatched uncertainty', *Internatinal Journal of Automation and Control*, Vol. 16, Nos. 3/4, pp.272–287 https://doi.org/10.1504/IJACC.2022.10046266.

Zhou, Y., Zhi, G., Chen, W., Qian, Q., He, D., Sun, B. and Sun, W. (2022a) 'A new tool wear condition monitoring method based on deep learning under small samples', *Measurement*, Vol. 189, p.110622 https://doi.org/10.1016/j.measurement.2021.110622.

Zhou, Y., Kumar, A., Prakash, C., Vashishtha, G., Tang, H. and Xiang, J. (2022b) 'A novel entropy-based sparsity measure for prognosis of bearing defects and development of a sparsogram to select sensitive filtering band of an axial piston pump', *Measurement*, Vol. 203, p.111997 https://doi.org/10.1016/j.measurement.2022.111997.

Zuo, X., Liu, J., Wang, X. and Liang, H. (2017) 'Adaptive PID and model reference adaptive control switch controller for nonlinear hydraulic actuator', *Mathematical Problems in Engneering*, Vol. 17, Article ID: 6970146, pp.1–15 https://doi.org/10.1155/2017/6970146.